

Time Scale of Fission at High Angular Momentum

A. Gavron

Los Alamos National Laboratory, Los Alamos, New Mexico 87545

and

J. R. Beene, B. Cheynis, R. L. Ferguson, F. E. Obenshain, F. Plasil, and G. R. Young

Oak Ridge National Laboratory, Oak Ridge, Tennessee 37830

and

G. A. Petitt

Georgia State University, Atlanta, Georgia 30303

and

M. Jääskeläinen and D. G. Sarantites

Washington University, St. Louis, Missouri 63130

and

C. F. Maguire

Vanderbilt University, Nashville, Tennessee 37235

(Received 18 May 1981)

Spectra of neutrons emitted in coincidence with evaporation residues and fission fragments have been measured in the (192 MeV) $^{12}\text{C} + ^{158}\text{Gd}$ and (176 and 239 MeV) $^{20}\text{Ne} + ^{150}\text{Nd}$ reactions. At the two lower energies, several neutrons are evaporated prior to fission. At the highest bombarding energy essentially all the neutrons are evaporated by the fragments indicating that at high angular momentum, the fission process is rapid compared to the time scale for neutron evaporation.

PACS numbers: 25.85.-w, 25.70.Fg, 24.75.+i

The behavior of the fission barrier in nuclear systems at high angular momenta has been the subject of several theoretical¹ and experimental^{2,3} investigations. In general, evaporation residue and fission cross sections are reproduced by statistical-model calculations^{4,5} using the rotating-liquid-drop (RLD) model¹ fission barriers reduced by approximately 20%. For angular momenta above the value at which the RLD barrier becomes zero, statistical model calculations of fission widths are inapplicable; it has been suggested⁶ that beyond this point, fission takes place on a time scale that is short with respect to characteristic particle evaporation times. This does not seem to be the case for some ^{40}Ar -induced reactions⁷ in which α -particle emission attributed to evaporation was found to precede fission.

We present here for the first time direct evidence for the onset of fast fission as the angular momentum of the system increases. The compound nucleus ^{170}Yb was chosen for this study due to the detailed previous studies of its various properties.^{5,8,9} Approximately 1-mg/cm² targets of ^{158}Gd were bombarded with 192-MeV ^{12}C produced at the Oak Ridge Isochronous Cyclotron.

Likewise, a target of ^{150}Nd was bombarded with 176- and 239-MeV ^{20}Ne beams. The excitation energies and critical angular momenta for fusion (calculated using the Bass potential¹⁰) are, respectively, 169 MeV ($l_{\text{crit}} = 72$), 135 MeV ($l_{\text{crit}} = 79$), and 191 MeV ($l_{\text{crit}} = 99$). The value of l_{crit} for 176-MeV ^{20}Ne agrees (within errors) with that obtained by Halbert *et al.*¹¹ Neutrons were detected in coincidence with evaporation residues (ER) and fission fragments (FF) using ten encapsulated NE-213 liquid scintillators. The general experimental setup is similar to that described in Ref. 9: FF were detected in a 50- μm -thick ΔE detector and identified by their characteristic locus on a two-dimensional plot of their time of flight (times against the cyclotron beam pulse) versus energy. An additional E detector behind it was used to veto particles that penetrated the ΔE detector. Because of the poor time resolution (~ 3 nsec) and short flight path (6.5 cm) it was not possible to analyze the mass and kinetic energy distributions. The ΔE detector subtended an in-plane angle between 18° and 30° , and an out-of-plane angle of $\pm 2.8^\circ$. ER were identified at $\pm 6^\circ$ as described in Ref. 9; likewise,

details of the neutron energy determination and detection efficiency calculation are presented there. An additional constraint on the neutron detection efficiency is imposed by the left-right symmetry of the neutron spectra in coincidence with ER (when summed over the two ER detectors⁹). Accordingly, deviations of more than 10% from symmetry in the neutron spectra in coincidence with FF are attributed to neutron emission from the fragments.

Typical neutron spectra are presented in Figs.

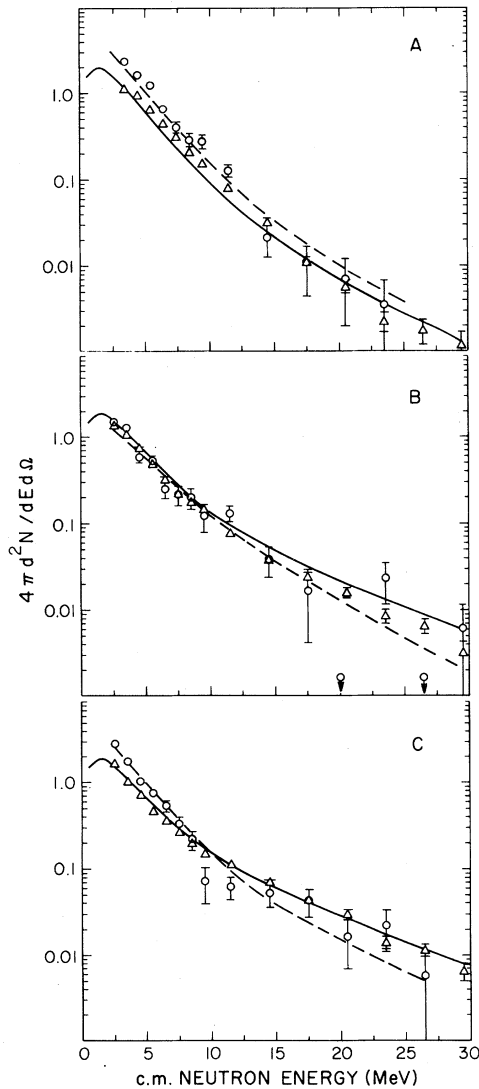


FIG. 1. Neutron spectra in the 192-MeV $^{12}\text{C} + ^{158}\text{Gd}$ reaction. Triangles, spectra in coincidence with ER; circles, in coincidence with FF. Full line, model fit to ER coincidence data; dashed line, model fit to FF coincidence data. Curves A, B, and C refer to angles of -138° , -55° , and 34° , respectively.

1 and 2 for the 192-MeV ^{12}C and 239-MeV ^{20}Ne reactions. The three angles we have chosen for graphic presentation here are -138° (curves A), -55° (curves B), and $+34^\circ$ (curves C); negative angles are on the opposite side of the beam with respect to the FF detector. Curves A and C are approximately collinear with the FF, while curve B is approximately perpendicular to the FF axis. Spectra in coincidence with ER (triangles) have two components: an evaporation spectrum isotropic in the c.m. system having a characteristic temperature of ~ 2 MeV and a nonequilibrium component, forward peaked in the c.m. system with a characteristic temperature of ~ 4 MeV. (These temperatures are deduced from a moving-

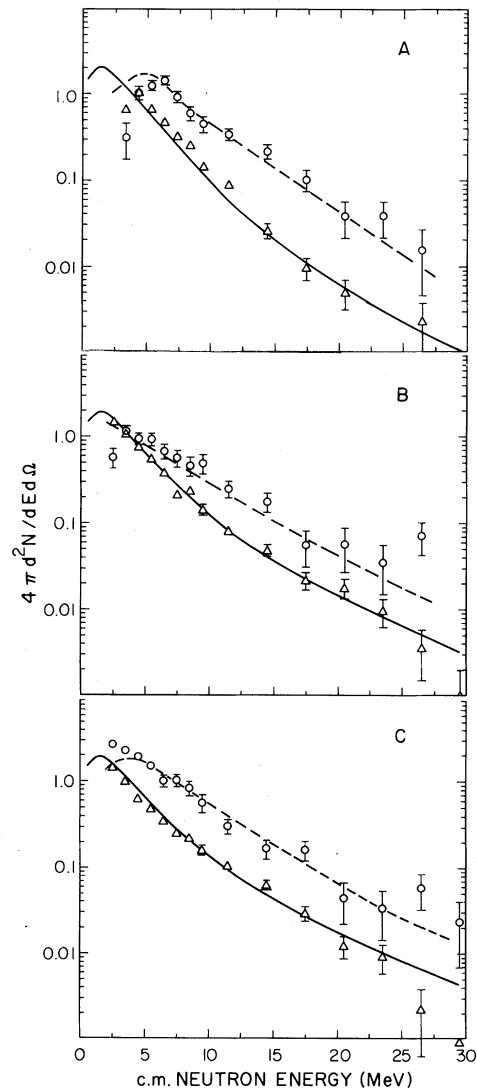


FIG. 2. Neutron spectra in the 239-MeV $^{20}\text{Ne} + ^{150}\text{Nd}$ reaction. Symbols have the same meaning as in Fig. 1.

source model fit⁹—the full line is the result of such a fit.) The circles depict neutron spectra in coincidence with FF. Considering Fig. 1, curve *B* (79° with respect to the fission detector direction) we see that there is essentially no difference between neutron spectra in coincidence with ER and in coincidence with FF at this angle. Identical comparisons can be made with other neutron detectors off the fission axis which are not presented here for lack of space. Neutron spectra in the direction of the fission axis (Fig. 1, curves *A* and *C*) show an excess of neutrons at low energies in coincidence with FF, compared to spectra in coincidence with ER; this excess is attributed to neutron emission from the moving fission fragments, while the majority of neutrons are emitted from the intermediate system. The fact that this excess is noticeable only at low energies and only around the direction of the fragments points to a small fraction of neutron emission for the FF and to a low fragment temperature. Similar conclusions can be drawn from the neutron spectra in the 176-MeV ²⁰Ne reaction. Neutron spectra obtained in the 239-MeV ²⁰Ne reaction (Fig. 2) present very different features: a neutron excess in coincidence with FF at all neutron energies, which is more pronounced in the direction of the fragments (Fig. 2, curves *A* and *C*) but also evident perpendicular to the fragment direction (Fig. 2, curve *B*). These results are compatible with a large fraction of neutrons emitted from high-temperature FF.

The neutron spectra were evaluated quantitatively as follows: Spectra in coincidence with ER were fit using the moving source parametrization⁹ (full lines in Figs. 1 and 2). An additional source—neutron evaporation from the moving FF—was employed in fitting spectra in coincidence with FF. The following assumptions were made about the fission process: The mass distribution symmetric, Gaussian shaped; FWHM (full width at half maximum)-28 amu for 192-MeV ¹²C and 176-MeV ²⁰Ne, -44 amu for 239-MeV ²⁰Ne.⁶ The average kinetic energy, 113 MeV was taken from the systematics of Viola,¹² and the width of the total kinetic energy distribution was assumed to be 18 MeV. Varying the widths does not have a significant effect on the results. The available excitation energy was split between the fragments in proportion to their mass. The neutron spectrum in the fragments' frame of reference was obtained for different excitation energies using a modified version of code JULIAN.⁵ In all, three parameters were varied in order to fit the neu-

tron spectra in coincidence with FF: The multiplicity of nonequilibrium neutrons, the multiplicity of neutrons evaporated from the compound system (the shapes were obtained previously from the fit to spectra in coincidence with ER), and the total excitation energy available to the two fragments. The resulting values are consistent with the total energy available. The parameters were varied to obtain reasonable agreement with all the (ten) measured neutron spectra. The errors quoted are estimates of the range of parameters in which equally acceptable fits are obtained. Results of the fitting procedure are presented in Fig. 3 as a function of l_{crit} .¹⁰ The FF temperatures plotted there are obtained from the evaporation calculations as

$$T = -[d \ln(E)/dE]^{-1} \quad (1)$$

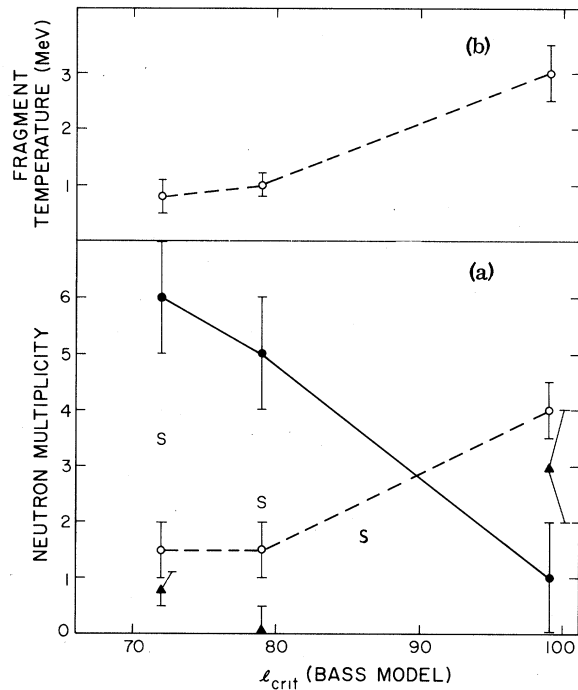


FIG. 3. Neutron multiplicities and fragment temperature obtained in model fit, as a function of l_{crit} (Ref. 10), summarizing all three reactions. (a) Triangles, number of nonequilibrium neutrons preceding fission; full circles, number of evaporated neutrons preceding fission; hollow circles, number of neutrons emitted from each fission fragment. S, results of statistical-model calculations of the multiplicity of evaporated neutrons preceding fission. The point at $86\hbar$ depicts the calculated result when the RLD barrier goes to zero for $l = l_{crit}$. (b) Temperature of fission fragments obtained from the model fit.

for large E . $N(E)$ is the neutron spectrum in the fragment frame of reference. Spectra obtained by these calculations are presented as a broken line in Figs. 1 and 2; both the shape and the angular distribution of the spectra are reproduced quite well.

Considering Fig. 3, we observe a sharp drop in the number of neutrons preceding fission, and a parallel increase in the neutron multiplicity from the fragments, as l_{crit} increases above 80. Neglecting excitation energy dependence (which is estimated to be small relative to angular momentum effects²⁻⁵) and considering the average pre-fission neutron multiplicity of 5 ± 1 for partial waves up to $79\hbar$, we have to assume that the pre-fission neutron multiplicity is zero above $(78 \pm 6)\hbar$ in order to obtain the experimental result of 1 ± 1 for partial waves up to $99\hbar$. For comparison the RLD barrier¹ goes to zero at $86\hbar$.

The results for 239-MeV ^{20}Ne are similar to those for strongly damped collisions (e.g., Ref. 13)—most of the excitation energy is dissipated by neutron evaporation from the fragments. We conclude that the fission process is a very rapid one at high angular momentum—somewhat shorter than 2×10^{-21} sec estimated for neutron evaporation.⁵ One possible explanation is the presence of “fast fission,” a decay mode short lived relative to compound-nucleus decay.¹⁴

In addition to the experimental results, Fig. 3 contains statistical model predictions⁵ for the number of pre-fission neutrons in the 192-MeV ^{12}C and 176-MeV ^{20}Ne reactions ($l_{\text{crit}} = 72$ and 79 , respectively). The calculations predict multiplicities considerably lower than experimental values. We note that the parameters used in the calculation were specifically adjusted to fit ^{170}Yb .⁵ We infer that fission at these angular momenta is slow even compared to statistical model predictions. Similarly a comparatively large number of neutrons preceding fission was obtained by Fraenkel *et al.*¹⁵ for low-energy (and low angular momentum) actinide fission. We can inter-

pret this suppression of fission in various ways: (1) At high excitation energies, the level density at the saddle point reflects the RLD fission barrier whereas at lower excitation energies the nuclear system can sense shell corrections.^{16, 17} If these corrections lower the fission barrier relative to the RLD barrier (e.g., to 80% of the RLD value^{2, 4, 5}) the fission probability will increase significantly at the end of the evaporation cascade. (2) If the coupling between the fission degree of freedom and the single-particle degrees of freedom is weak,¹⁸ neutron emission will be enhanced in the initial stages of deexcitation. (3) Deformation effects at high angular momentum¹⁹ could modify the decay sequence.

¹S. Cohen, F. Plasil, and W. J. Swiatecki, *Ann. Phys. (N.Y.)* **82**, 557 (1974).

²F. Plasil *et al.*, *Phys. Rev. Lett.* **45**, 333 (1980), and references therein.

³H. Oeschler *et al.*, *Phys. Rev. C* **22**, 546 (1980).

⁴F. Plasil and M. Blann, *Phys. Rev. C* **11**, 508 (1975); F. Plasil, ORNL ALICE, Oak Ridge National Laboratory Report No. ORNL-KM-6054, 1977 (unpublished).

⁵A. Gavron, *Phys. Rev. C* **21**, 230 (1980).

⁶C. Lebrun *et al.*, *Nucl. Phys. A* **321**, 207 (1979).

⁷D. Logan *et al.*, *Phys. Rev. C* **22**, 1080 (1980).

⁸D. G. Sarantites *et al.*, *Phys. Rev. C* **14**, 2138 (1976).

⁹A. Gavron *et al.*, *Phys. Rev. C* (to be published).

¹⁰R. Bass, *Phys. Rev. Lett.* **39**, 265 (1977).

¹¹M. L. Halbert *et al.*, *Phys. Rev. C* **17**, 155 (1978).

¹²V. Viola, *Nucl. Data* **1**, 39 (1966).

¹³Y. Eyal *et al.*, *Phys. Rev. C* **21**, 1377 (1980).

¹⁴C. Gregoire, C. Ngô, and B. Remaud, *Phys. Lett.* **99B**, 17 (1981); B. Borderie *et al.*, *Z. Phys.* **299**, 263 (1981).

¹⁵Z. Fraenkel *et al.*, *Phys. Rev. C* **12**, 1809 (1975).

¹⁶F. C. Williams, G. Chan, and J. R. Huizenga, *Nucl. Phys. A* **187**, 225 (1972).

¹⁷L. G. Moretto, in *Proceedings of the Third IAEA Symposium on Physics and Chemistry of Fission, Rochester, New York, 1973* (International Atomic Energy Agency, Vienna, Austria, 1974), p. 329–364.

¹⁸P. Grangé and H. A. Weidenmüller, *Phys. Lett.* **96B**, 26 (1980).

¹⁹M. Blann, *Phys. Rev. C* **21**, 1770 (1980).